

# Electron confinement and optical enhancement in Si/SiO<sub>2</sub> superlattices

Pierre Carrier,<sup>1</sup> Laurent J. Lewis,<sup>1,\*</sup> and M. W. Chandre Dharma-wardana<sup>2</sup>

<sup>1</sup>*Département de Physique et Groupe de Recherche en Physique  
et Technologie des Couches Minces (GCM), Université de Montréal,*

*Case Postale 6128, Succursale Centre-Ville, Montréal, Québec, Canada H3C 3J7*

<sup>2</sup>*Institute for Microstructural Sciences, National Research Council, Ottawa, Canada K1A 0R6*

(Dated: March 22, 2022)

We have performed first-principles calculations of Si/SiO<sub>2</sub> superlattices in order to examine their electronic states, confinement and optical transitions, using linearized-augmented-plane-wave techniques and density-functional theory. Two atomic models having fairly simple interface structure are considered; they differ in the way dangling bonds at interfaces are satisfied. We compare our first-principles band structures with those from tight-binding calculations. The real and imaginary parts of the dielectric function are calculated at the Fermi-Golden-rule level and used to estimate the absorption coefficients. Confinement is confirmed by the dispersionless character of the electronic band structures in the growth direction. Optical enhancement is shown to exist by comparing the direct and indirect transitions in the band structures with the related transitions in bulk-Si. The role played by the interface on the optical properties is assessed by comparing the absorption coefficients from the two models.

PACS numbers: 78.66.Jg, 68.65.+g, 71.23.Cq

## I. INTRODUCTION

Informatics and telecommunications are the driving forces behind the development of new photonic devices.<sup>1</sup> Such devices can be assembled from a wide variety of materials; among these, silicon is probably the most prevalent, although it suffers from having an indirect band gap. Direct band-gap materials such as GaAs, InP, and many other III-V and II-VI semiconductors, are efficient electron-photon energy converters. However they are costly for large-scale applications, and would be less interesting if full Si-based photonics were possible. These considerations have lead to considerable efforts towards the development of new types of Si-based materials having direct energy gap in the visible (viz. 1.5 to 3 eV),<sup>2</sup> suitable for photo-diodes and lasers, as well as solar-cell applications.

The simultaneous discovery by Canham<sup>3</sup> and Lehmann and Gösele<sup>4</sup> of intense luminescence in porous silicon ( $\pi$ -Si) has opened up new horizons for Si-based materials.  $\pi$ -Si can be regarded as consisting of long and thin nanowires,<sup>5</sup> forcing the electronic states to be confined within the finite dimension of the nanostructures. The shift of the luminescence spectrum towards the blue with decreasing nanowire size<sup>3</sup> suggests that the confinement of the electronic states might be responsible for the visible luminescence. Unfortunately, most forms of  $\pi$ -Si are unstable, lasting only a few hours before a strong decrease of the luminescence efficiency is observed. This instability has sometimes been attributed to the volatile Si-H bonds at the surface.<sup>4</sup> Annealing under nitrogen and oxygen has been suggested as a means of stabilizing the structures; however, the annealed material has weaker luminescence than the parent  $\pi$ -Si. Layered polysilanes (Si<sub>6n</sub>H<sub>6</sub>) also exhibit optical properties similar to  $\pi$ -Si. Uehara et al<sup>6</sup> have performed first-principles calculations

of layered polysilanes structures and showed that porous Si may be akin to thin Si<sub>6</sub>H<sub>6</sub> sheets.

As a perhaps more promising avenue, confinement can also be achieved in superlattices (SLs) — or quantum wells — as well as quantum wires and quantum dots. Lu et al have reported enhanced luminescence in the visible part of the spectrum of Si/SiO<sub>2</sub> SLs fabricated by molecular beam epitaxy (MBE),<sup>7</sup> and a blue shift was observed when the thickness of the Si layers was reduced from 6 to 2 nm. In contrast to  $\pi$ -Si, Si/SiO<sub>2</sub> SLs present the advantage of being stable, with no significant decrease of the luminescence observed with time.

Motivated by these promising experimental observations, and to provide insight into the microscopic physics associated with the luminescence efficiency of SL-based devices, we undertook a detailed, first-principles investigation of the electronic and optical properties of Si/SiO<sub>2</sub> SLs. Silicon and SiO<sub>2</sub> are both already standard components of MOSFETs and other devices. SiO<sub>2</sub> has an energy gap of  $\sim 9$  eV; Si has an indirect gap of  $\sim 1.1$  eV. Thus, the electrons are confined by the SiO<sub>2</sub> barriers within the silicon quantum wells. Luminescence, however, is not determined solely by confinement since the nature of the energy gap is also important. The possibility of creating a direct energy gap in a SL can be discussed in simplified terms within the concept of Brillouin zone folding:<sup>8</sup> The periodicity of a SL,  $d$ , being larger than that of the constituent lattices,  $a_0$ , the Brillouin zone gets folded to dimension  $\pi/d$  instead of  $\pi/a_0$ , which may bring the indirect minimum of the conduction band to the  $\Gamma$ -point and thus produce an effectively direct energy-gap material. “Quasi-direct” energy gaps were so obtained in Si/Ge superlattices;<sup>9</sup> however, there was little enhancement in the optical properties.

In this work, we examine the luminescence properties of Si/SiO<sub>2</sub> SLs using model structures and first-principles

methodology. Transmission electron microscopy reveals that in Si/SiO<sub>2</sub> SLs, both Si and SiO<sub>2</sub> layers are amorphous.<sup>7</sup> Amorphous structures are however not easily amenable to quantum calculations. Here, we assume crystalline phases for both the Si and SiO<sub>2</sub> slabs. This is further motivated by the need to study simple ideal systems as benchmarks, and in particular to determine how the difference in the interface affects the optical properties. We however note that crystalline-Si based SLs have very recently been fabricated.<sup>10</sup>

Two simple model structures for Si/SiO<sub>2</sub> SLs are considered: (i) The double-bonded model (DBM) of Herman and Batra,<sup>11</sup> shown in Fig. 1(a); here the Si and SiO<sub>2</sub> layers are arranged so as to minimize the lattice mismatch and have relatively high symmetry, and the dangling bonds at the interfaces are saturated by the addition of a single double-bonded oxygen atom. (ii) A bridge-oxygen model (BOM), shown in Fig. 1(b), where the interface dangling bonds are saturated by adding an oxygen atom to bridge two Si bonds. Full details of the models are given in Section II A.

The electronic properties of both the DBM and the BOM have been studied already within an empirical tight-binding framework by Tit and Dharma-wardana,<sup>12</sup> who observed the bands along the high-symmetry lines of the BZ parallel to the  $k_z$  axis to be essentially dispersionless, in agreement with the present calculations. However, the band gaps were found to be direct in both models, in contradiction with our results. The DBM has been studied from first principles by Punkkinen et al.<sup>13</sup> using a full-potential linear-muffin-tin orbital approach. However, no other interface-structure was examined and thus the effect of changing the interface could not be assessed; further, the optical properties were not calculated. Kageshima and Shiraishi have also used first-principles methods to examine different models for the Si-SiO<sub>2</sub> interface in oxide-covered Si slabs,<sup>14</sup> but the SL geometry was not examined. Their calculations indicate that the interface plays an important role in the light-emitting properties of the system and that, in particular, interfacial Si-OH bonds are possibly related to the observed luminescence. Here we present results for the electronic structure, the dielectric function and the absorption coefficient of both the DBM and the BOM, and focus on a comparison between the two models.

## II. COMPUTATIONAL DETAILS

### A. Model structures

SLs can be fabricated by MBE;<sup>15</sup> a major advantage of this technique, as compared to others, is that it gives sharper interfaces. In the case of Si/SiO<sub>2</sub> SLs, Lu et al.<sup>7</sup> report an interface thickness of about 0.5 nm, while the thickness of the SiO<sub>2</sub> and Si layers vary between 2 and 6 nm. Here we assume that the interfaces are perfectly sharp.

The model Si/SiO<sub>2</sub> SL structures are constructed by alternating layers of crystalline (diamond) silicon and crystalline SiO<sub>2</sub> in the ideal  $\beta$ -cristobalite structure, viz. with a Si-O-Si bond angle of 180° (space group Fd $\bar{3}$ m). The (experimental) lattice constants are 5.43 and 7.16 Å, respectively, with therefore a lattice mismatch of 32%. The mismatch can be reduced to less than 7% by rotating the Si unit cell by an angle of  $\pi/4$  so that the diagonal of the Si-diamond structure fits, approximately, the cubic edge of the  $\beta$ -cristobalite unit cell. The superposition of the Si and SiO<sub>2</sub> layers gives rise to dangling bonds on some of the interface Si atoms. These can be satisfied in different ways. In the DBM, this is done by adding a single O atom onto one of the Si atoms. The resulting unit cell has 23 atoms [cf. Fig.1(a)] and dimensions 5.43 Å in the  $x-y$  plane and  $5.43 \times (1 + \sqrt{2}) = 13.11$  Å in the  $z$  (growth) direction. In this model, the Si-Si and Si-O distances, 2.35 and 1.66 Å, respectively, are realistic, but the double-bonded oxygen Si=O is not found in naturally occurring silicates. In the BOM, Fig. 1(b), an oxygen atom saturates two dangling bonds provided by two different Si atoms; this model contains 21 atoms. Here the Si-O-Si angle is the usual 144° and the length of the Si-O bonds at the interface is 2.02 Å, i.e., somewhat longer than found in nature. No energy relaxation of the models have been carried out. However, as will be discussed in section III C, we found gap states to be present in the BOM; in order to understand this, we investigated two other variants of the BOM, having Si-O-Si angles of 109 and 158°, respectively.

The Brillouin zone for the SL, along with that for c-Si, is depicted in Figure 2. The principal symmetry axes are indicated: the  $Z - \Gamma$ ,  $X - R$  and  $M - A$  directions correspond to possible growth directions where confinement is expected to occur, as discussed below.

### B. First-principles calculations

The electronic-structure calculations were carried out with the WIEN97 code,<sup>16</sup> which uses the all-electron, full-potential, linearized-augmented-plane-wave (LAPW) method,<sup>17</sup> within the framework of density-functional theory<sup>18,19</sup> in the local-density approximation (LDA).<sup>20</sup> Thus, the core states in the (spherical) atomic region are described using an atomic basis, while the delocalized states in the interstitial region are expanded in plane waves which are correctly formulated to account for the core region. The Kohn-Sham (KS) basis inside the atomic spheres is expressed as an angular-momentum expansion:

$$\psi(\vec{k}_n, \vec{r}) = \sum_{l,m} \left[ A_{lm}^n u_l(r, E_l) + B_{lm}^n \frac{\partial u_l}{\partial E} \Big|_{E=E_l} \right] Y_{lm}(\hat{r}).$$

Here the energy  $E_l$  is calculated and fixed at the first cycle of the self-consistent-field calculation. The KS equations are solved for a grid of  $\vec{k}$  points as discussed below.

The integration of the radial secular equations was performed on a radial mesh containing 581 points. The radius of the spheres for silicon and oxygen atoms were set at 0.87 and 0.79 Å, respectively, and an energy cutoff of  $-7.1$  Ry was used for separating core from valence electrons. This generated 11 149 plane waves and the matrix size for the eigenvalue problem contained 5581 elements. These two parameters correspond to an angular momentum cutoff of 7.5 (see Singh<sup>17</sup> for further details), a value which ensures proper energy convergence of the solution.

The DBM has nine non-equivalent atoms while the BOM has eight. The irreducible wedge of the Brillouin zone is obtained after four symmetry operations, which reduces considerably the computational load. The supercell in the  $z$  direction being 3 times longer than in the  $x$  or  $y$  directions, only 181  $\vec{k}$  points were necessary to achieve convergence of the electronic energies. However, in order to ensure convergence of the wave functions needed to set up the optical matrix, the density of  $\vec{k}$  points had to be doubled. Integration of the Brillouin zone was performed using the tetrahedron method and Broyden density mixing. The self-consistent calculations were performed in parallel mode (using four processors) on a Silicon Graphics Origin 2000 computer system. About 10 cycles were necessary to get convergence of the energy to about  $10^{-4}$  Ry.

### III. RESULTS AND DISCUSSION

#### A. Band structures

The electronic band structures along the high symmetry axes of the tetragonal Brillouin zone (cf. Fig.2) for the two models are plotted in Fig. 3, together with the densities of states (DOS). For the BOM, unless otherwise noted, the interfacial Si-O-Si angle is the normal  $144^\circ$ . The confinement in the  $z$ -direction can already be inferred from the essentially dispersionless character of the bands along the three symmetry axes which are parallel to the axis of the SL, namely  $X-R$ ,  $Z-\Gamma$  and  $M-A$ ; this was also observed by Punkkinen et al.<sup>13</sup> Thus, optical transitions between bands lying in the growth direction are favored by the confinement.

The DOS of the two models differ strongly in the region of the gap, with an isolated conduction band clearly visible in the gap of the BOM which is absent in the DBM. The only difference between the two models lies in the way that the interfacial dangling bonds are fixed; the gap state in the BOM is thus connected to the bridge-bonded Si atom. The results, evidently, are sensitive to the way that the interface is formed, either in experiment, or in a theoretical model. This question will be discussed in more detail in section III C.

The effect of the confinement in both models is clearly visible from the DOS. If we ignore the gap state in the BOM for the moment, the DOS at the Fermi level has a step-function-like threshold, as opposed to bulk-silicon

which is known<sup>21</sup> to have a threshold depending on the photon energy  $\hbar\omega$  as  $(\hbar\omega - E_g)^{1/2}$ , where  $E_g$  is the gap energy. Higher transition probabilities are thus expected in Si/SiO<sub>2</sub> SLs.

Figure 4 zooms on the band structure of the two models near the Fermi level. The numerical values of the various possible transition energies are given in Table I. For the DBM, the valence-band maximum (VBM) is at the  $\Gamma$  point but the conduction band minimum (CBM) is in between the  $\Gamma$  and  $X$  points (labeled  $\Gamma X/2$  in Table I), giving an indirect gap of 0.81 eV. For the BOM, the VBM is at  $X$  while the CBM is at  $Z$ , giving an almost null (0.01 eV) indirect band gap. However, it should be remembered that the energy gaps are significantly underestimated in the LDA and other implementations of the DFT. Thus the bulk-Si LDA energy gap is 0.49 eV, about 0.6 eV below the true value of 1.1 eV. Better (but non-rigorous) estimates for the DBM and the BOM energy gaps would thus be 1.4 and 0.6 eV, respectively. The unusually low value for the energy gap of the BOM is an indication that the lowest conduction band is really a gap state. If this state [“CB1” in Fig.4(b)] is assumed to be an unphysical artifact of the model, and temporarily ignored, the indirect gap of 1.49 eV gets corrected to  $\sim 2.1$  eV. Thus, the energy gap would be in the near infrared or in the red, consistent with experiment.<sup>7,22,23</sup>

The dispersionless character of the bands in the growth direction provides evidence of the confinement effect, as noted above. However, confinement alone is not sufficient to explain the enhancement of the optical properties; comparison of the direct and indirect transitions for the two models can clarify this question. For the DBM, the direct transitions at  $\Gamma$  and  $\Gamma X/2$  have energies of 0.98 eV and 0.84 eV, respectively, while the  $\Gamma - \Gamma X/2$  indirect transition (i.e., the band gap) costs 0.81 eV. Thus the *smallest direct-indirect gap* (SDIG) in the LDA for the DBM is a mere 0.03 eV (0.84 – 0.81 eV). For the BOM (if the “CB1” gap state is ignored), the direct transitions at  $X$  and  $Z$  have energies of 2.19 and 1.87 eV, respectively, compared to 1.49 eV for the  $Z-X$  indirect transition, for a SDIG of only 0.35 eV. These numbers can be compared to the corresponding ones for bulk silicon (in the LDA): the direct transition at the  $\Gamma$  point has energy 2.52 eV while the direct transition at the CBM (near  $3/4\Gamma X$ ) costs 3.20 eV. The indirect band gap is 0.49 eV, so that the SDIG in this case is  $\sim 2.0$  eV. This is *much larger* than that for the DBM and the BOM. The latter, as a consequence, has much better optical properties than bulk Si. It is also clear that the DBM will have better optical properties than the BOM (see section III D) since the SDIG of the DBM is smaller than that of the BOM.

#### B. Comparison with tight-binding calculations

It is instructive to compare the present results to those obtained for the same model systems by Tit and Dharma-wardana<sup>24</sup> within a tight-binding (TB) framework. In a

TB description,<sup>25</sup> the wavefunctions are expressed as linear combinations of atomic orbitals and the exact many-body Hamiltonian is replaced by a parametrized Hamiltonian matrix whose eigenvalues and eigenvectors yield the energies and the wavefunctions of the corresponding electron levels. The size of the numerical problem is determined by the number of atomic orbitals chosen to describe the valence electrons, and about 4 or 5 orbitals per atom are typically used. This allows the study of much larger systems than is possible in first-principles calculations. It is therefore important to assess the validity of TB models in order to re-calibrate and improve the TB parametrization. Indeed, the parameters are typically fitted to experimental data or first-principles calculations for the *pure* crystalline phases. For mixed systems, e.g., a SL, the parameters are assumed to be transferable except for simple adjustments of energy reference or scaling to bond lengths, etc.

An important parameter entering TB calculations is the valence-band offset (VBO), which is the difference in energy between the VBM of the two materials constituting the SL.<sup>26</sup> In their calculations, Tit and Dharmawardana assumed a VBO of 3.75 eV, based on the experimental offset between Si and amorphous SiO<sub>2</sub>. However, this value need not be appropriate to the idealized DBM and BOM models.

In Fig. 5(a) we compare the LDA band structure for the DBM with the TB results of Tit and Dharmawardana,<sup>24</sup> who used a VBO value of 3.75 eV; Fig. 5(c) is the corresponding plot for the BOM. The agreement with this particular value of the VBO is, at best, qualitative; this may indicate that the choice of VBO needs revision. In order to assess this, we have done new TB calculations using different VBO values. By adjusting as closely as possible the valence band structures to the TB ones, better values of the VBO were found to be 0.0 eV for the DBM and 1.0 eV for the BOM; the results are indicated in Fig. 5(b) and (d), where the band gaps from LDA are adjusted to the TB values to help comparison. For the BOM, the gap state “CB1” from LDA coincides well with the first conduction band obtained from TB, except in the  $X$ - $Z$  region of the BZ. The first-principles “CB2”, in contrast, is somewhat higher than found from the TB calculations. Thus, while not perfect, the agreement with the first-principles calculations improves significantly with these new VBO values.

### C. Gap states in the BOM

In view of the presence of a gap state in the BOM — labeled “CB1” in Fig. 4 — and in order to assess the role of the interface on the electronic properties, other possibilities for the interfacial Si–O–Si angle were considered: (i) 109°, corresponding to positioning the oxygen atom on a normal silicon site of the Si lattice; here,  $d_{\text{Si-O}} = 2.35$  Å; (ii) 144° which corresponds to the experimental value of the Si–O–Si angle, used in the calculations discussed

above, yielding  $d_{\text{Si-O}} = 2.02$  Å; and finally (iii) 158°, a value obtained by relaxing the oxygen atom position, and which corresponds to a (local) energy minimum; in this case,  $d_{\text{Si-O}} = 1.96$  Å. The “normal” Si–O distance in silica is 1.61 Å, which cannot be accommodated by the crystalline silicon lattice in the BOM.

Figure 6 shows the band structures for the three cases; here we consider only the  $X - R - Z$  direction, wherein lies the energy gap. Evidently, the precise value of the interfacial Si–O–Si bond angle, and corresponding Si–O bondlength, have a sizeable effect on the band structure. In fact, the 158°-BOM is, within the LDA, a metal if CB1 is not assumed to be a gap state, as discussed earlier. Likewise, the 144°-BOM is nearly metallic. These results indicate that the acceptable range of interfacial Si–O–Si angles, and the consequent longer than “normal” Si–O distances, are probably essential issues in explaining the luminescence in Si/SiO<sub>2</sub> SLs.

### D. Optical properties

The Kohn-Sham calculations provide matrix elements and joint densities of states necessary for the calculation of the complex dielectric function  $\vec{\epsilon} = \vec{\epsilon}_r + i\vec{\epsilon}_i$ . The absorption coefficient  $\alpha$ , which can then be deduced from  $\vec{\epsilon}$  as a function of the photon energy (see below), provides a detailed picture of one aspect of the optical properties of the material. In principle, the luminescence requires a knowledge of the excited states of the system, with electrons occupying the conduction band. Such states are not available from DFT calculations. Further, the electrons in the conduction band are associated with holes in the valence band. For low carrier concentrations, the screening is weak and hence exciton formation occurs.<sup>27</sup> This many-body effect is also required for a complete description of luminescence. Such calculations require, e.g., the solution of the Bethe-Salpeter equation for the electron-hole pair (see Chang et al., Ref. 28) and are still prohibitive even for our model structures. Excitonic effects will thus be neglected here.

As already noted, the band gaps are underestimated by LDA-DFT and this has to be corrected if the absorption thresholds are to be realistic. In practice, this can be done to a reasonable approximation by rigidly shifting all the conduction bands to the appropriate energy. However, we remain within the DFT framework and calculate the absorption in the Fermi-golden-rule approximation. Also, we assume that the emission spectrum is similar to the absorption spectrum and neglect excitonic effects. In spite of these approximations, the main mechanisms of luminescence enhancement — the effects arising from the joint density of states and the matrix elements — would be correctly captured.

Using the program written by Abt et al.<sup>29</sup> as part of the WIEN97 package,<sup>16</sup> the imaginary part of the dielectric

function has been determined; it is given by:

$$\epsilon_i^\alpha(\omega) = \left( \frac{4\pi e^2}{m^2 \omega^2} \right) \sum_{v,c} \int \frac{2d\vec{k}^3}{(2\pi)^3} |\langle c\vec{k} | \mathcal{H}^\alpha | v\vec{k} \rangle|^2 \\ < f_{v\vec{k}} (1 - f_{c\vec{k}}) \delta(E_{c\vec{k}} - E_{v\vec{k}} - \hbar\omega),$$

where  $f_{v\vec{k}}$  is the Fermi distribution and  $\mathcal{H}^\alpha$  is the  $\alpha$ -component of the electron-radiation interaction Hamiltonian in the Coulomb gauge; it corresponds to the probability per unit volume for a transition of an electron in the valence band state  $|v\vec{k}\rangle$  to the conduction band state  $|c\vec{k}\rangle$  to occur. From Kramers-Kronig relations one then deduces the real part  $\epsilon_r$ .<sup>21</sup> The dielectric function  $\vec{\epsilon}$  is defined as the square of the complex refractive index  $\vec{n} = n_r + in_i$ , so that

$$\alpha(E) = 4\pi \frac{E}{hc} n_i = 4\pi \frac{E}{hc} \left[ \frac{(\epsilon_r^2 - \epsilon_i^2)^{1/2} - \epsilon_r}{2} \right]^{1/2},$$

with  $c$  the speed of light in vacuum,  $h$  Planck's constant, and  $E$  the photon energy.

Figure 7 shows the  $z$ -component of the absorption coefficients for the DBM and for the three different variations of the BOM. We also give, for comparison, the corresponding curves for silicon and for the ideal  $\beta$ -cristobalite  $\text{SiO}_2$  structures. The energy gaps are those directly from the LDA; correcting the gaps would only affect the position of the onset, but not the general aspect. The absorption coefficient for the two models are similar. This similarity is, to a large extent, a “zone folding” effect, as the two model structures have identical  $z$ -dimensions (the growth axis). However, closer inspection reveals that the DBM has better absorption properties than the three BOMs: the onset of absorption is sharper, and occurs earlier in the DBM than in all the BOM. This is consistent with the band structure analysis above that showed the SDIG to be smaller in the DBM than in the BOM ( $\sim 0.03$  vs  $\sim 0.35$  eV), implying a larger transition probability for the former than the latter.

In addition, the calculated SDIG for the BOM with an interfacial Si–O–Si angle of  $109^\circ$  is 0.18 eV — the band gap (or the indirect transition) being 1.53 eV while the direct transition between  $X$  and  $Z$  are 2.06 eV and 1.71 eV respectively — in between the SDIG for the DBM and the BOM with  $144^\circ$ . This is in agreement with the absorption curves of Fig. 7, where the absorption onset is higher for the DBM, lower for the BOM with  $109^\circ$  and then even lower for the BOM with  $144^\circ$  or  $158^\circ$ . The last two give similar absorption curves as can be seen from Fig. 7.

Thus, the four models (the DBM and the BOM with bond angles  $109^\circ$ ,  $144^\circ$  and  $158^\circ$ ), which differ only

by their interface definition, give rather different optical properties. The onset of the absorption curve in the BOM with Si–O–Si angles of  $144^\circ$  and  $158^\circ$  do not differ that much from the one obtained from bulk-Si, while the DBM and the BOM with  $109^\circ$ , viz. the BOM with higher Si–O bondlengths at the interface, give better optical properties. This is additional indication that the interfacial atomic structure has to be connected to the optical enhancement in the SLs, in agreement with Kageshima's analysis.<sup>14</sup> Likewise, it can be concluded from Fig. 7 that bulk Si has poor optical properties compared to the SLs, since the onset of absorption lags behind that for the two SLs and the SDIG is much larger.

#### IV. CONCLUDING REMARKS

We have used first-principles calculations to (i) study the electronic and optical properties of Si/SiO<sub>2</sub> SL models and (ii) examine the applicability of tight-binding calculations for these systems.

Concerning the second point, our results indicate that, for both models, the VBO value of 3.75 eV used in TB calculations is excessive. In addition, the direct-transition nature of the gap from the TB calculations is incorrect. The present calculations indicate that the band gap in both models is indirect (albeit quasi-direct), in the red or infrared region of the spectrum. Confinement is further confirmed by the essentially dispersionless character of the electronic band structures in the growth direction (cf. Figs 3 and 4). Our calculations indicate, also, that the SLs have enhanced optical properties as compared to pure Si.

The influence on the optical properties of the Si–SiO<sub>2</sub> interface has been assessed from the absorption coefficient. This quantity depends critically on the details of the interfacial structure. Realistic models are thus essential for determining the electronic and optical properties. We are presently studying improved models for this system.<sup>30</sup>

*Acknowledgments* – It is a pleasure to thank Gilles Abramovici, Ralf Meyer and Michel Côté for useful discussions. This work is supported by grants from the Natural Sciences and Engineering Research Council (NSERC) of Canada and the “Fonds pour la formation de chercheurs et l'aide à la recherche” (FCAR) of the Province of Québec. We are indebted to the “Réseau québécois de calcul de haute performance” (RQCHP) for generous allocations of computer resources.

\* To whom correspondence should be addressed;  
e-mail: laurent.lewis@umontreal.ca

<sup>1</sup> G.A. Lampropoulos and R.A. Lessard, *Applications of*

- Photonic Technology*, SPIE, **3491** (1998).
- <sup>2</sup> P. Zhang, V.H. Crespi, E. Chang, S.G. Louie, and M.L. Cohen, *Nature* **409**, 69 (2001).
  - <sup>3</sup> L.T. Canham, *Appl. Phys. Lett.* **57**, 1046 (1990).
  - <sup>4</sup> V. Lehmann, U. Gösele, *Appl. Phys. Lett.* **58**, 856 (1991).
  - <sup>5</sup> S.-F. Chuang, S.D. Collins, R.L. Smith, *Appl. Phys. Lett.* **55**, 675 (1989).
  - <sup>6</sup> K. Uehara, J.S. Tse, *Chem. Phys. Lett.* **301**, 474 (1990).
  - <sup>7</sup> Z.H. Lu, D.J. Lockwood, J.-M. Baribeau, *Nature* **378**, 258 (1995).
  - <sup>8</sup> U. Gnitzmann, K. Clausecker, *Appl. Phys.* **3**, 9 (1974).
  - <sup>9</sup> T.P. Pearsall, J. Bevk, L.C. Feldman, J.M. Bonar, J.P. Mannaerts, *Phys. Rev. Lett.* **58**, 729 (1987).
  - <sup>10</sup> Z.H. Lu, private communication.
  - <sup>11</sup> F. Herman, I.P. Batra, *The Physics of SiO<sub>2</sub> and its interfaces* ed. by S.T. Pantelides, (Pergamon, Oxford, 1978).
  - <sup>12</sup> N. Tit, M.W.C. Dharma-wardana, *J. Appl. Phys.* **86**, 1 (1999).
  - <sup>13</sup> M.P.J. Punkkinen, T. Korhonen, K. Kokko, I.J. Värynen, *Phys. Stat. Sol. (b)* **214**, R17 (1999).
  - <sup>14</sup> H. Kageshima, K. Shiraishi, *Mat. Res. Soc. Symp. Proc.* **486**, 337 (1998).
  - <sup>15</sup> M.A. Herman, H. Sitter, *Molecular Beam Epitaxy* (Springer-Verlag, Berlin, 1989).
  - <sup>16</sup> P. Blaha, K. Schwarz, and J. Luitz, WIEN97, Vienna University of Technology 1997. [Improved and updated Unix version of the original copyrighted WIEN code, which was published by P. Blaha, K. Schwarz, P. Sorantin, S.B. Trickey, *Comput. Phys. Commun.* **59**, 399 (1990).]
  - <sup>17</sup> D.J. Singh, *Planewaves, pseudopotentials and the LAPW method* (Kluwer Academic, Norwell, 1994).
  - <sup>18</sup> P. Hohenberg, W. Kohn, *Phys. Rev.* **136**, B864 (1964).
  - <sup>19</sup> W. Kohn, L.J. Sham, *Phys. Rev.* **140**, A1133 (1965).
  - <sup>20</sup> M.C. Payne, M.P. Teter, D.C. Allan, T.A. Arias, and J.D. Joannopoulos, *Rev. Mod. Phys.* **64**, 1045 (1992).
  - <sup>21</sup> P.Y. Yu, M. Cardona, *Fundamentals of Semiconductors* (Springer, New-York, 1996).
  - <sup>22</sup> V. Mulloni, R. Chierchia, C. Mazzoleni, G. Pucker, L. Pavesi, P. Bellutti, *Philos. Mag. B* **80**, 705 (2000).
  - <sup>23</sup> S.V. Novikov, J. Sinkkonen, O. Kilpelä, S.V. Gastev, *J. Vac. Sci. Technol. B* **15**, 1471 (1997).
  - <sup>24</sup> N. Tit, and M.W.C. Dharma-wardana, *Physics Letters A* **254**, 233 (1999).
  - <sup>25</sup> D.A. Papaconstantopoulos, *Handbook of the Band Structure of Elemental Solids* (Plenum, New York, 1986).
  - <sup>26</sup> R. Williams, *J. Vac. Sci. Technol.* **14**, 1106 (1977).
  - <sup>27</sup> R.S. Knox, *Theory of excitons in Solid State Physics*, (Academic Press, New-York, 1963).
  - <sup>28</sup> E.K. Chang, M. Rohlfing, S.G. Louie, *Phys. Rev. Lett.* **85**, 2613 (2000).
  - <sup>29</sup> R. Abt, C. Ambrosch-Draxl, P. Knoll, *Physica B* **194-196**, 1451 (1994).
  - <sup>30</sup> M. Tran, N. Tit, M.W.C. Dharma-wardana, *Appl. Phys. Lett.* **75**, 4136 (1999).

TABLE I: Possible (LDA-DFT) transition energies (in eV) for the two models (DBM and BOM with Si-O-Si interfacial angle of 144°). CB1, CB2, and VB refer to the first and second conduction band, and the valence band, respectively. For the DBM,  $\Gamma X/2$  designates the conduction band minimum, which lies approximately half-way between  $\Gamma$  and  $X$  points (cf. Fig. 4). The lowest direct and indirect transitions are listed; the energy gaps, which are indirect, are indicated in boldface. For the BOM, CB1 can be viewed as a gap state (see text), and the “true” LDA-gap is therefore 1.49 eV; for the DBM, this gap state is absent, i.e., CB1 is the true lowest band, and the LDA gap is 0.81 eV.

	BOM		DBM	
	$X$	$Z$	$\Gamma$	$\Gamma X/2$
CB2	2.1870	1.4932	—	—
CB1	1.7447	0.0142	0.0781	0.8050

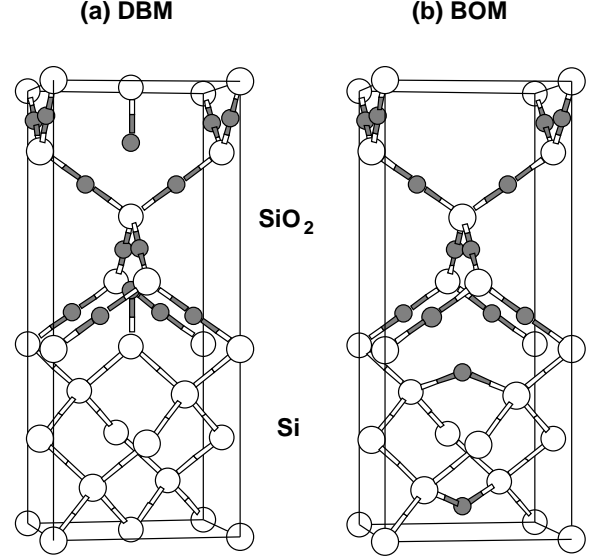


FIG. 1: The two model structures considered in the present study: (a) the DBM, which contains 23 atoms (13 Si and 10 O), and (b) the BOM, which contains 21 atoms (11 Si and 10 O atoms). Both unit cells are rectangular, of size  $5.43 \times 5.43 \times 13.11 \text{ \AA}^3$ . The two models differ only by their Si-SiO<sub>2</sub> interface.

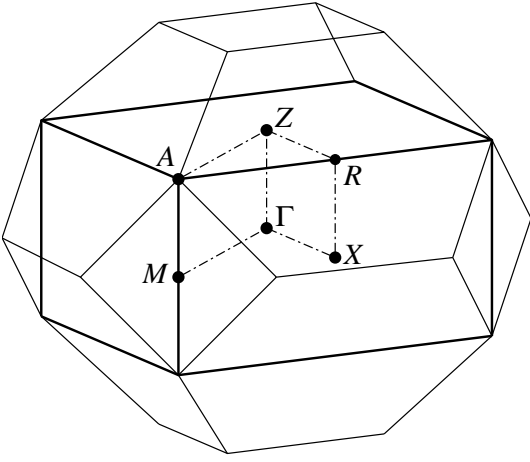


FIG. 2: Brillouin zone for the SL compared to that for the diamond structure. The principal axes of symmetry used in the electronic structures calculations are also shown.

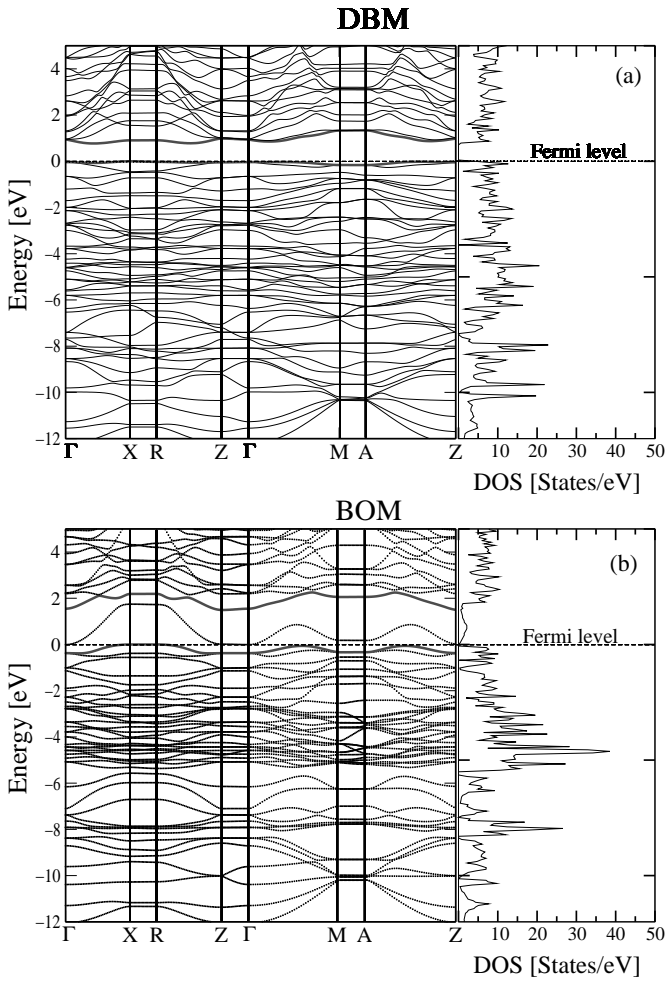


FIG. 3: Band structure and DOS for (a) the DBM and (b) the BOM.

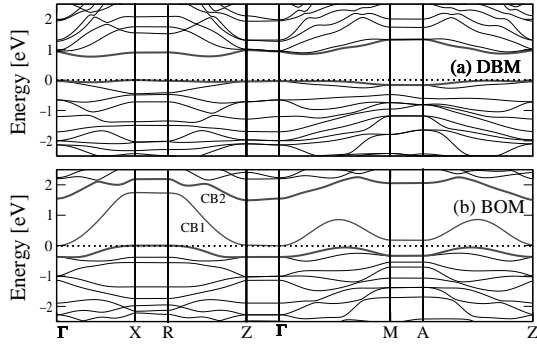


FIG. 4: Detail of the band structure near the Fermi level for the DBM and the BOM.

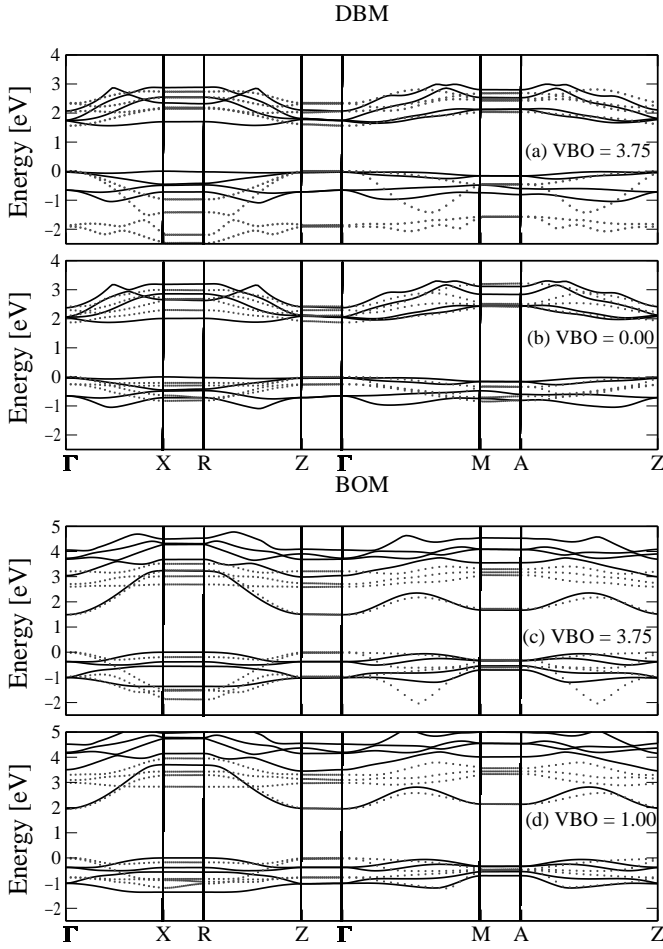


FIG. 5: Comparison between TB (dotted lines) and first-principles (full lines) band structures for the two models, for two different values of the VBO: (a) 3.75 eV and (b) 0.0 eV for the DBM; (c) 3.75 eV and (d) 1.0 eV for the BOM. The LDA energy gaps were “manually” set to the gap from TB calculations in order to facilitate the comparison.



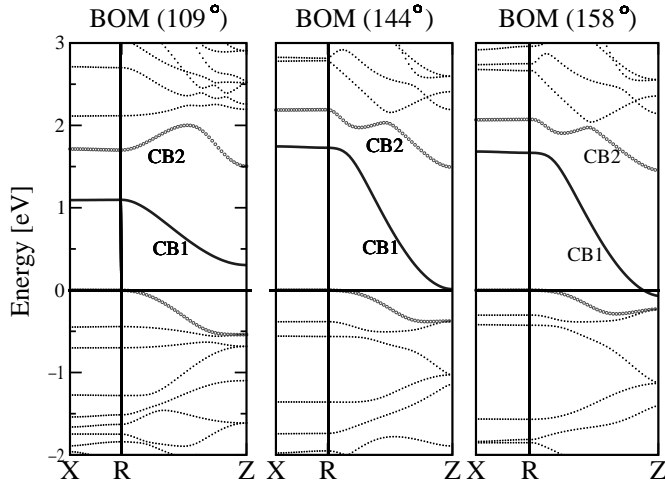


FIG. 6: Band structure of the BOM having three different interfacial Si-O-Si angles (as indicated).

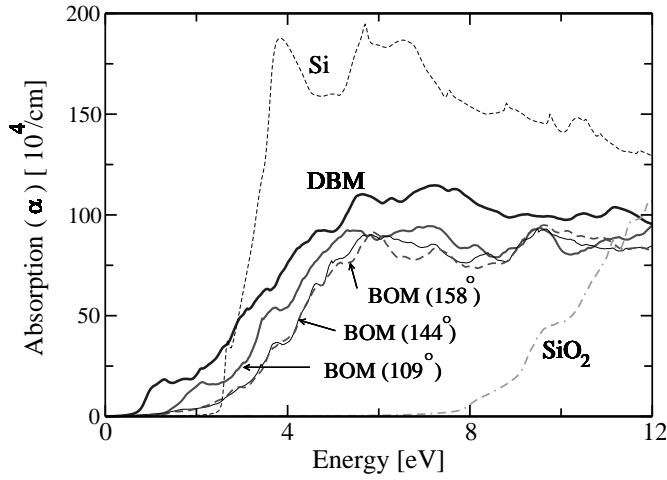


FIG. 7: Absorption curves for the two models compared to bulk Si and ideal  $\beta$ -cristobalite  $\text{SiO}_2$ . The three BOM angles correspond to the interfacial Si-O-Si angle in the model. The BOM curves for  $144^\circ$  and  $158^\circ$  overlap almost exactly; the full line corresponds to an angle of  $144^\circ$  while the dotted line corresponds to an angle of  $158^\circ$ .